Electronic Supporting Information for

Monolithic and flexible fluoropolymer film microreactor for organic synthetic applications

Jin-Oh Kim,[a,b] Heejin Kim,[a] Dong-Hyeon Ko,[a] Kyoung-Ik Min,[a] Do Jin Im,[c] Soo-Young Park[b]* and Dong-Pyo Kim[a]*

[a] Department of Chemical Engineering, Pohang University of Science and Technology, , Pohang, South Korea.

[b] Department of Polymer Science and Engineering, Kyungpook National University, Daegu, South Korea

[c] Department of Chemical Engineering, Pukyong National University, Busan, South Korea

E-mail: dpkim@postech.ac.kr

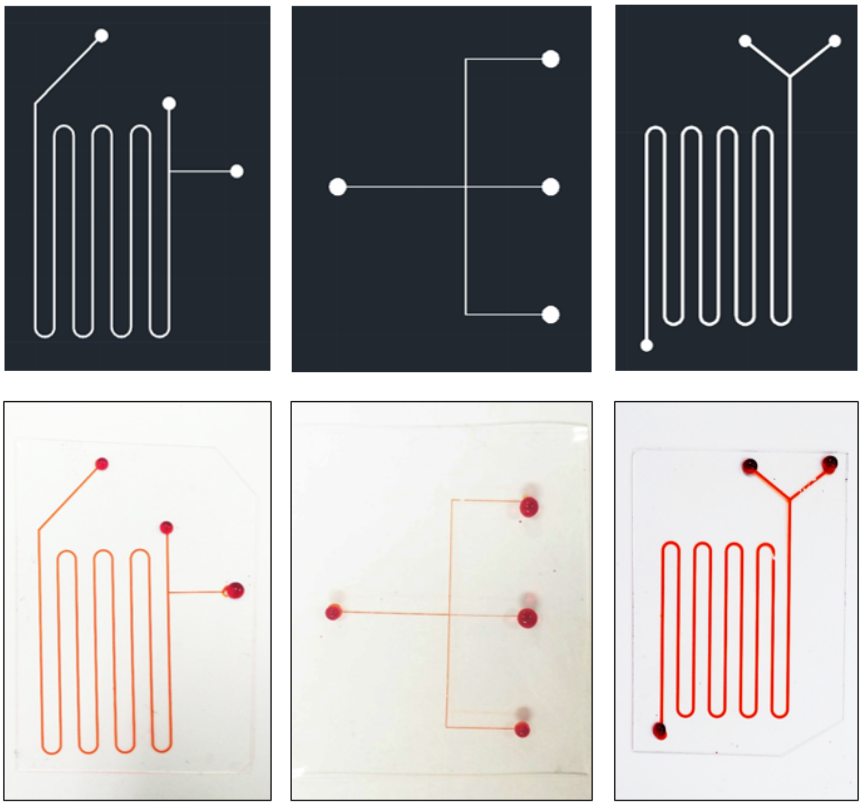

Figure S1. a) Various kinds of microchannel CAD design, b) optical images of the fabricated fluoropolymer film microreactors

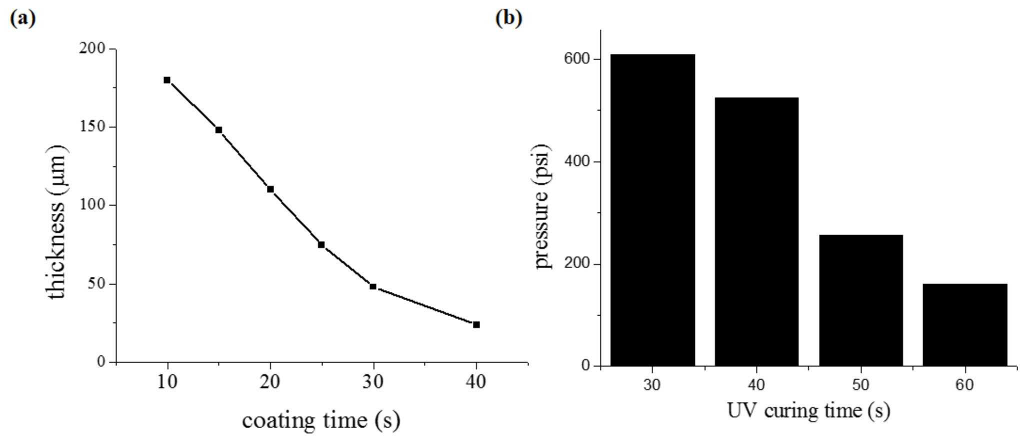

Figure S2. (a) Dependence of spin-coated film thickness of fluoropolymer resin on spin-coating time under spinning rate at 500 rpm. (b) Different burst pressures of the fluoropolymer film microreactors when the plain film on flat Si wafer was cured at different partial curing times, and the film was bonded by conformal contact with the patterned film that was cured for 1 min UV exposure.

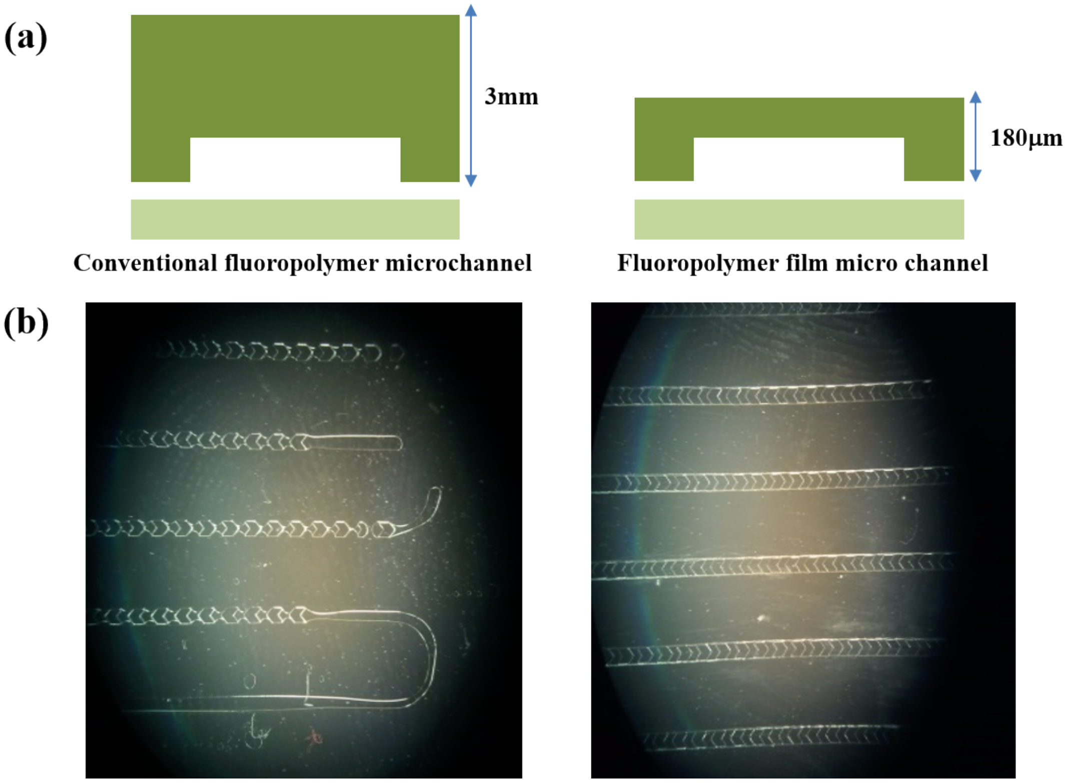

Figure S3. Comparative bonding reliability of the cured and patterned fluropolymer laminates with different thickness in the microreactor fabrication (300 μm width, 50 μm height, 30 cm length). (a) Low bonding reliability by rigid and thick (3 mm) laminate with no intimate contact. (b) High bonding reliability by thin (180 μm) laminate with conformal and intimate contact.

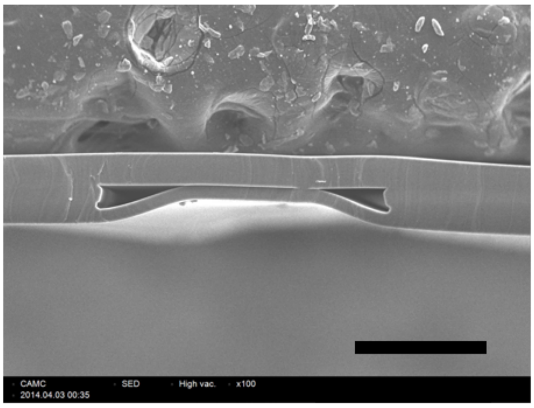

Figure S4. SEM image of the collapsed PDMS microchannel (500 μm width, 50 μm height) fabricated by thin film fabrication method. Scale bar: 300 μm.

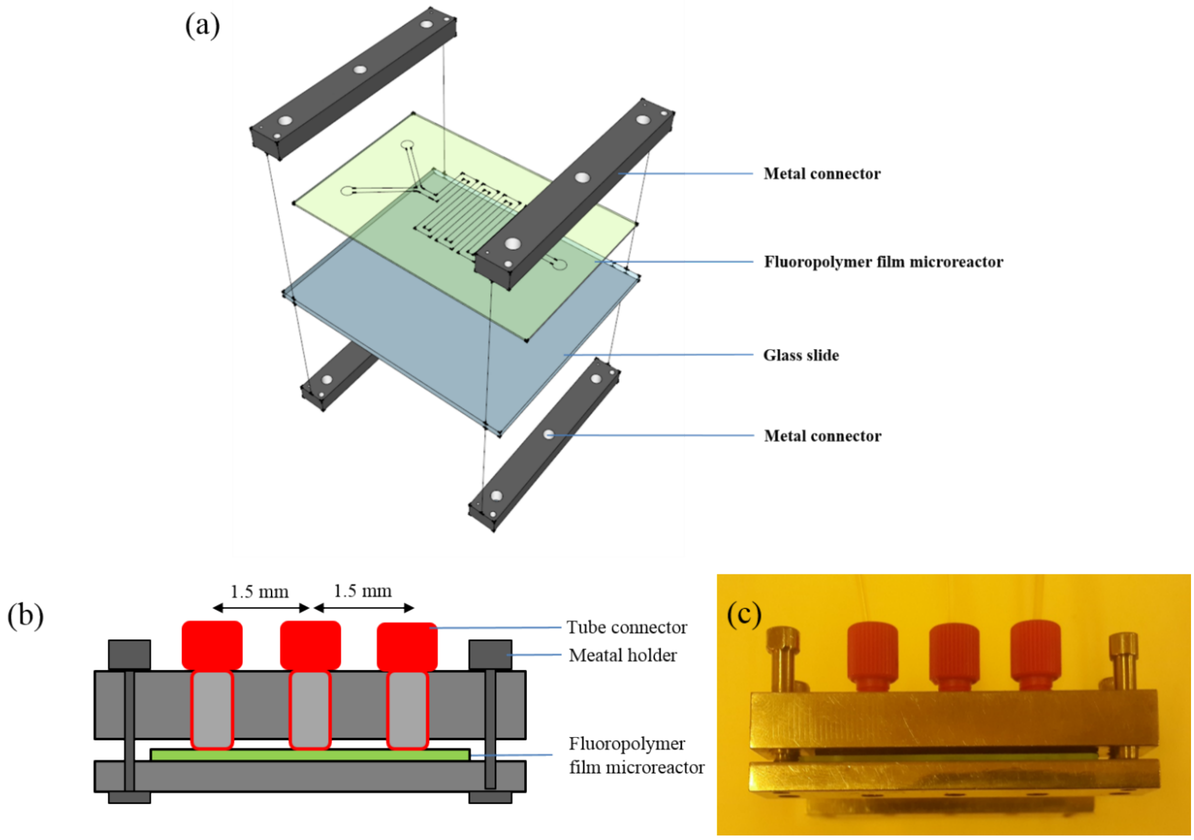

Figure S5. Metal clamping system to interface tubing with the fluoropolymer film microreactor. (a) 3 dimensional scheme, (b) cross-sectional illustration, and (c) optical image.

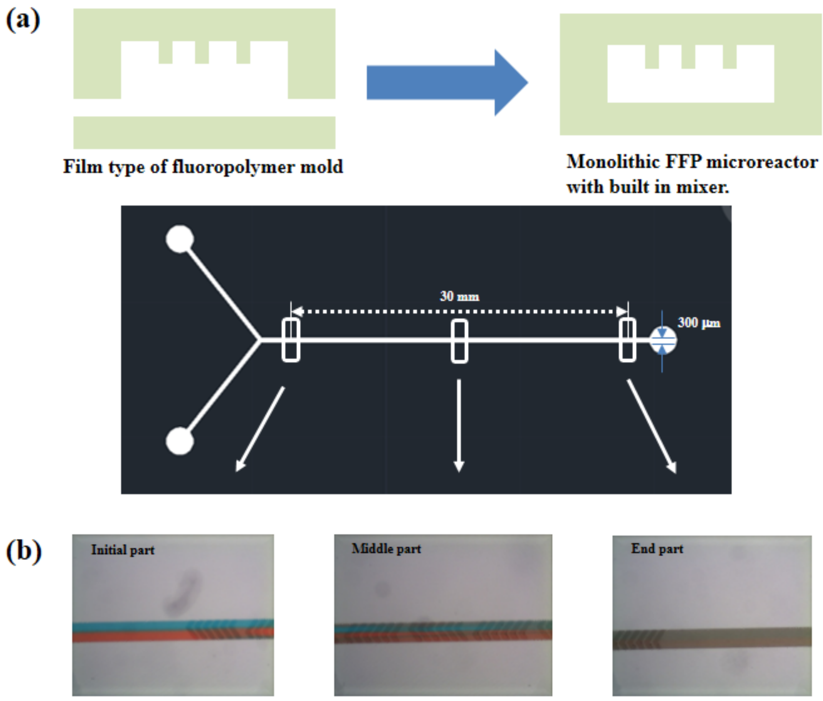

Figure S6. A monolithic and flexible fluoropolymer film microreactor embedded with built-in staggered herringbone mixer pattern. (a) Fabrication scheme of the built-in micromixer (300 µm x 50 µm x 30 mm). (b) Optical microscopic images on mixing efficiency at initial part (0 to 2.5 mm, left image), middle part (13.7 to 16.2 mm, center image) and end part (27.5 to 30 mm, right image) with a total flow of 10 µL/min.

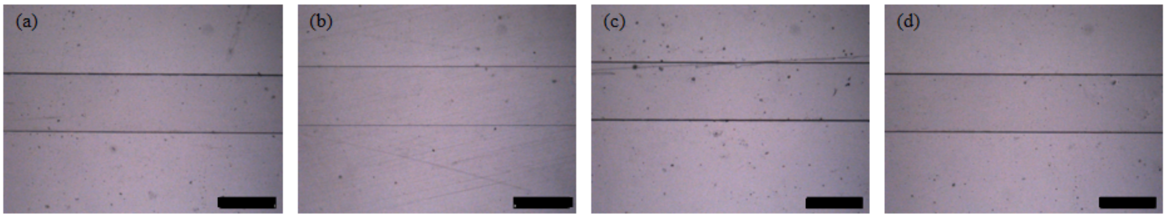

Figure S7. Durability test of fabricated microchannel for organic solvents showed that there was no significant damage on the microchannel. Several kinds of solutions were flowed into the microchannel with 500 μm width for 1 hr: (a) water, (b) 65% strongly acidic nitric acid solution, (c) 40 wt% strongly basic methylamine solution, (d) neat chloroform.

Table S1. Comparison of swelling behaviour between PDMS and PFPE by soaking the rectangular pieces (1cm x 1cm x1mm) in a Soxhlet extractor for 12 hrs.

Solvent	PDMS at RT (%)	PFPE at RT (%)	PFPE at 60℃ (%)
Water	0.0	0.0	0.0
Dimethylsulfoxide	3.0	0.25	4.0
Acetonitrile	5.0	2.8	3.0
Dimethylformamide	6.2	4.2	5.0
Acetone	13.5	3.3	7.7
Benzene	43.6	1.8	4.2
Tetrahydrofuran	95.9	5.0	11.9
Hexane	112.0	1.2	0.9
Chloroform	127.5	6.6	14.6
Trichloroethylene	173.6	4.1	8.2
60% Nitric acid	Crack	2.2	Yellow wish

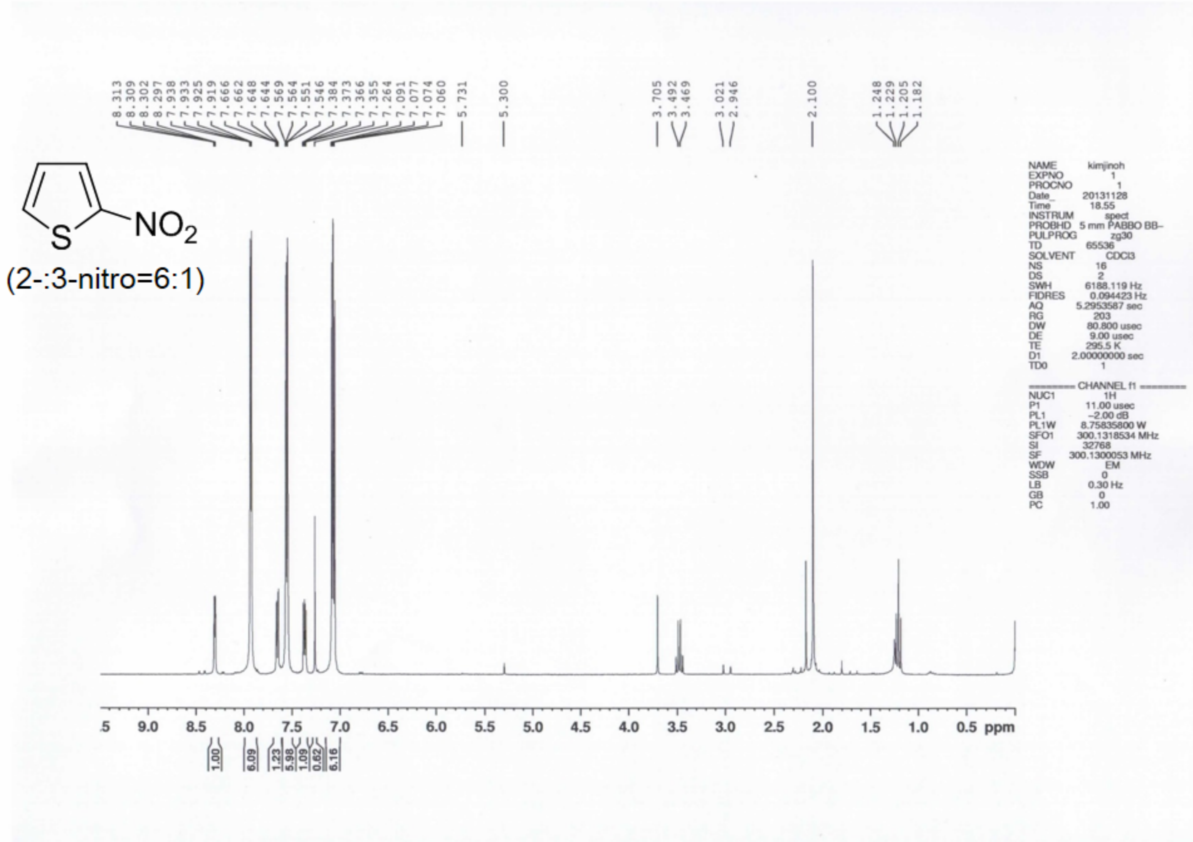

Figure S8. ^{1}H-NMR spectrum of (2-:3-) nitro- thiophene in $CDCl_3$

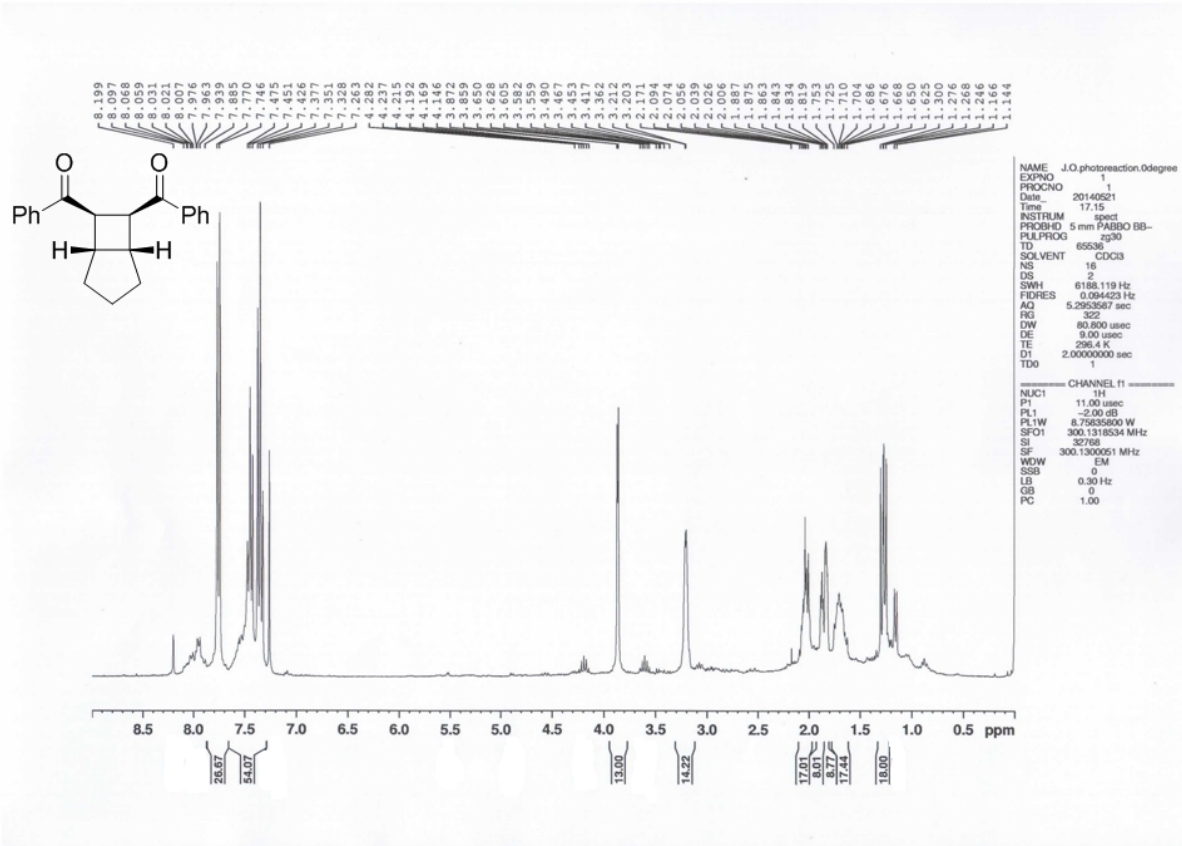

Figure S9. 1H-NMR spectrum of (1R,5S,6R,7S)-bicyclo[3.2.0]heptane-6,7-diylbis(phenylmethanone) in CDCl3